

Facile synthesis of Pd@ZnO core@shell nanoparticles for selective ethanol detection

Sonalika Agarwal^{a,*}, Sanjay Kumar^a, Eric Navarrete Gatell^b, Manoj Kumar^a, Eduard Llobet^b, Kamalendra Awasthi^{a,c,*}

^a Department of Physics, Malaviya National Institute of Technology Jaipur, Rajasthan 302017, India

^b MINOS-EMaS, Universitat Rovira i Virgili, Avda. Països Catalans 26, 43007 Tarragona, Spain

^c Materials Research Centre, Malaviya National Institute of Technology Jaipur, Rajasthan 302017, India



ARTICLE INFO

Article history:

Received 31 December 2020

Received in revised form 15 February 2021

Accepted 4 March 2021

Available online 9 March 2021

Keywords:

Core@shell

Pd@ZnO

Ethanol sensor

ABSTRACT

In this work, we reported a high-performance ethanol gas sensor based on novel Pd@ZnO core@shell nanoparticles (CSNPs). The Pd@ZnO CSNPs were synthesized by chemical method and characterized by XRD, TEM and EDS techniques. Gas sensing results demonstrated that Pd@ZnO CSNPs show high sensitivity and remarkable selectivity towards ethanol at 250 °C. The response value of Pd@ZnO CSNPs is 152, which is almost six times higher than the response value (27) of ZnO NPs at 250 °C. The mechanism of enhancement in sensing properties can be ascribed to the chemical and electronic sensitization effect of Pd NPs and also due to the unique core@shell structure. These characteristics may shed light on the development of a selective ethanol sensor based on Pd@ZnO CSNPs.

© 2021 The Authors. Published by Elsevier B.V. This is an open access article under the CC BY-NC-ND license (<http://creativecommons.org/licenses/by-nc-nd/4.0/>).

1. Introduction

Ethanol (C₂H₅OH) is one of the inflammable, colorless, and volatile organic compounds (VOCs), and has been widely investigated in the field of food & drink industry, biomedical productions, breath analysis, chemical industries, and traffic safety [1–3]. Yet, the long-term exposure to ethanol also affects human health and especially shows toxic effects on the central nervous system [4]. As it is widely used as a beverage, its consumption is one of the main reasons for traffic accidents due to drunk driving. Therefore, the detection of ethanol vapor in drunken drivers is not only of medical but also of social importance [5]. This leads to immense research efforts for the development of efficient gas sensors for ethanol with high sensitivity, good selectivity, and rapid response [6].

In recent decades, metal oxide semiconductors (MOS) have been widely reported as chemical sensing materials [7]. As a typical n-type metal oxide having a wide bandgap, zinc oxide (ZnO) is considered the most promising sensing material [8,9]. Nevertheless, the single component ZnO based gas sensors still suffer from poor selectivity, very particularly, cross-sensitivity to ambient moisture and long response and recovery times [10]. Several

approaches have been reported to solve the problem of cross-sensitivity such as engineering the morphology, modifying chemical composition by doping, and functionalization with noble metals [11].

Among them, noble metal@metal oxide semiconductor (M@MOS) core-shell nanostructures are becoming interesting and widely reported for gas sensing due to their unique shape, size, high catalytic activity, and controllable chemical and colloidal stability within the shell and charge transfer between core and semiconductor [12]. Recently, noble metal nanoparticles (such as Pd, Pt, Au and Ag) have been widely used in gas sensing applications due to their excellent catalytic properties [13,14].

Among the different metals cited above, Pd nanoparticles are the most suitable candidate for improving gas sensing properties of ZnO due to their good chemical stability, low orbital energy and high surface area [15]. Pd@ZnO core@shell nanostructures have not yet been widely explored for the detection of ethanol. So, the aim of the present study is the simple chemical synthesis of Pd@ZnO core@shell nanoparticles (CSNPs) and the investigation of their gas-sensing properties.

2. Experimental section

The Pd NPs, ZnO NPs, and Pd@ZnO CSNPs were synthesized by chemical method and detailed procedures are given in the supplementary material. The morphologies of sensing nanomaterials

* Corresponding authors.

E-mail addresses: sonalika.spsl@gmail.com (S. Agarwal), kawasthi.phy@mmit.ac.in (K. Awasthi).

were observed using high-resolution transmission electron microscopy (HRTEM, Tecnai G² 20 (FEI) S-TWIN). The crystallinity was studied by X-Ray diffraction (XRD, Panalytical XPert Pro X-ray diffractometer) using with Cu-K α 1 ($\lambda = 1.5406 \text{ \AA}$) radiation source. Energy dispersive spectrometry (EDS) of Pd@ZnO CSNPs was performed using a detector coupled to a field emission scanning electron microscope (FESEM, Nova Nano FE-SEM 450 FEI). The fabrication of gas sensing devices followed the methods discussed elsewhere [16] with few modifications (for details, see supplementary material).

3. Results and discussion

In the XRD patterns (Fig. 1), all the diffraction peaks can be indexed as the wurtzite hexagonal structure of ZnO and are given by standard data files (JCPDS file no. 01-079-0206). The sharp diffraction peaks show the good crystalline quality of Pd@ZnO CSNPs. However, no additional peak corresponding to metallic Pd was observed in the XRD pattern for Pd@ZnO CSNPs, which could be due to the small amount of Pd in Pd@ZnO, compared to Zn or O. No other impurity peaks were detected during XRD measurements, which confirms the high purity of the samples.

Fig. 2(a) shows the TEM image Pd nanoparticles with spherical shape and having an average diameter ranging from 10 to 15 nm. Fig. 2(b & c) displays the TEM images of spherical shape Pd@ZnO CSNPs with an average diameter of about 100–150 nm, where the single metal core of Pd and ZnO shell can be easily distinguished. The Fig. 2d (recorded after the heating process at 500 °C) shows no change in morphology with some shrinkage in diameter (ca. 100 nm and 80 nm, before and after calcination). It is also noticeable that core@shell structures have a highly porous surface after calcination, which is most beneficial for the good dispersion of the Pd and for preventing the sintering of Pd NPs. The SAED pattern of Pd@ZnO CSNPs is displayed in Fig. 2e and revealed their polycrystalline nature. On the other hand, the average diameter of pure ZnO is 80–120 nm, as illustrated in Fig. 2f. In addition, the presence of Pd, Zn, and O in the Pd@ZnO CSNPs was confirmed using EDS, shown in Fig. S1 and corresponding FESEM image is in the inset. The highly dispersive distribution of Pd, Zn, and O elements confirmed that no other impurities are present and established the formation of Pd@ZnO core@shell nanostructure.

The gas sensing properties of the Pd@ZnO CSNPs and ZnO NPs were investigated for various gases (ethanol, H₂, CO, and CO₂). The typical behavior of n-type semiconductor was revealed from

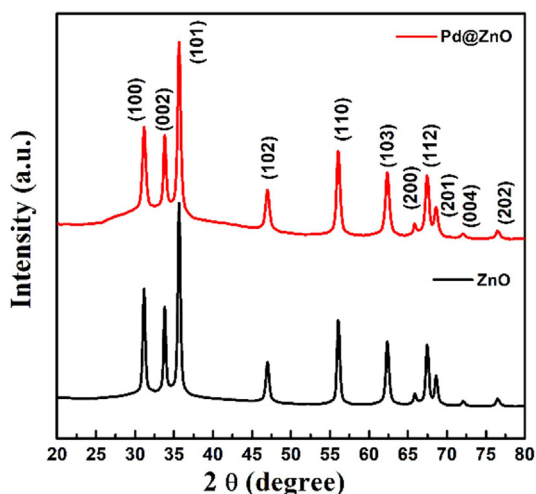


Fig. 1. XRD patterns of Pd@ZnO CSNPs and ZnO NPs.

Fig. 3(a) when exposed to ethanol (reducing gas). The response and recovery cycles of three pulses were repeated 5 times to test the repeatability of the sensor with increasing concentration of ethanol (5, 10, and 20 ppm) and results showed that the gas sensing measurements were highly repeatable. To optimize the working temperature, prepared sensing devices were tested at various temperatures i.e. 200 °C, 250 °C, and 300 °C. The temperature-dependent response of ZnO NPs and Pd@ZnO CSNPs sensor towards ethanol (20 ppm) is displayed in Fig. 3b. The response for both sensors is low at 200 °C and attained its maximum value at 250 °C, which may be due to achieving enough thermal energy to overcome the activation energy barrier for the reaction occurring during sensing [17]. By further increasing the temperature to 300 °C, the sensing response decreases, which may be due to exceeding the desorption rate of gas molecules than adsorption rate and causing the low utilization rate of the sensing material [18].

The maximum response value of 152 was achieved for Pd@ZnO whereas, for pristine ZnO, the response was 27. A nearly 6-fold increase in ethanol responsiveness for 20 ppm is obtained for core@shell nanoparticles at 250 °C, which could be attributed to the catalytic effect of Pd NPs [19]. Fig. 3(c) presents the response of both sensors toward ethanol at different concentrations at 250 °C. Results show that the Pd@ZnO CSNPs based sensors exhibited high response at each concentration in comparison to ZnO NPs and response increased with increasing concentration of gas. Furthermore, the Pd@ZnO CSNPs sensor was tested for ethanol (20 ppm), H₂ (200 ppm), CO (200 ppm), and CO₂ (200 ppm) at 250 °C (optimum working temperature), shown in Fig. 3(d). Among all analytes, the superior sensitivity and highest selectivity were obtained for Pd@ZnO CSNPs towards ethanol. The maximum response is 152 for 20 ppm ethanol whereas the response for H₂, CO, and CO₂ at 200 ppm is 3.59, 1.95, and 1.12, respectively, which is much lower than the response recorded for ethanol. This suggests that Pd@ZnO core@shell nanoparticles are suitable materials for ethanol detection.

ZnO follows a typical n-type semiconductor behavior and its sensing mechanism is as follows [20]. In presence of air, atmospheric oxygen gets adsorbed and being converted into ionic oxygen species by capturing electrons from the conduction band of the ZnO. As a result, a depletion layer is formed at the surface of the material and hence, the resistance of the material gets increased. When a reducing species such as ethanol reacts with adsorbed oxygen, trapped electrons are released back to the conduction band, which contributes to decrease its electrical resistance [21], as shown in Fig. 4(a). As reported by various researchers, the sensitivity of ZnO can be tuned by introducing catalytically active metals [22]. This enhancement in sensitivity may be attributed to the increased amount of oxygen species at the surface of ZnO and the formation of Schottky junction at interface of Pd and ZnO as shown in Fig. 4(b). Since Pd is a noble metal with effective catalytic activity, when it exists at the core, it provides an effective electronic and chemical sensitization effect to the sensing properties because of the symmetry in composition [23,24]. When oxygen molecules diffuse to the Pd nanoparticle surface, oxygen species are formed more effectively thus, a great enhancement in adsorbed oxygen is observed, which improves the sensitivity [25] of Pd@ZnO CSNPs.

4. Conclusions

In summary, an ethanol sensor based on Pd@ZnO core@shell nanoparticles was successfully developed and exhibited superior sensitivity, excellent selectivity, and remarkable repeatability. Significantly, almost a 6-fold increase in response value was observed

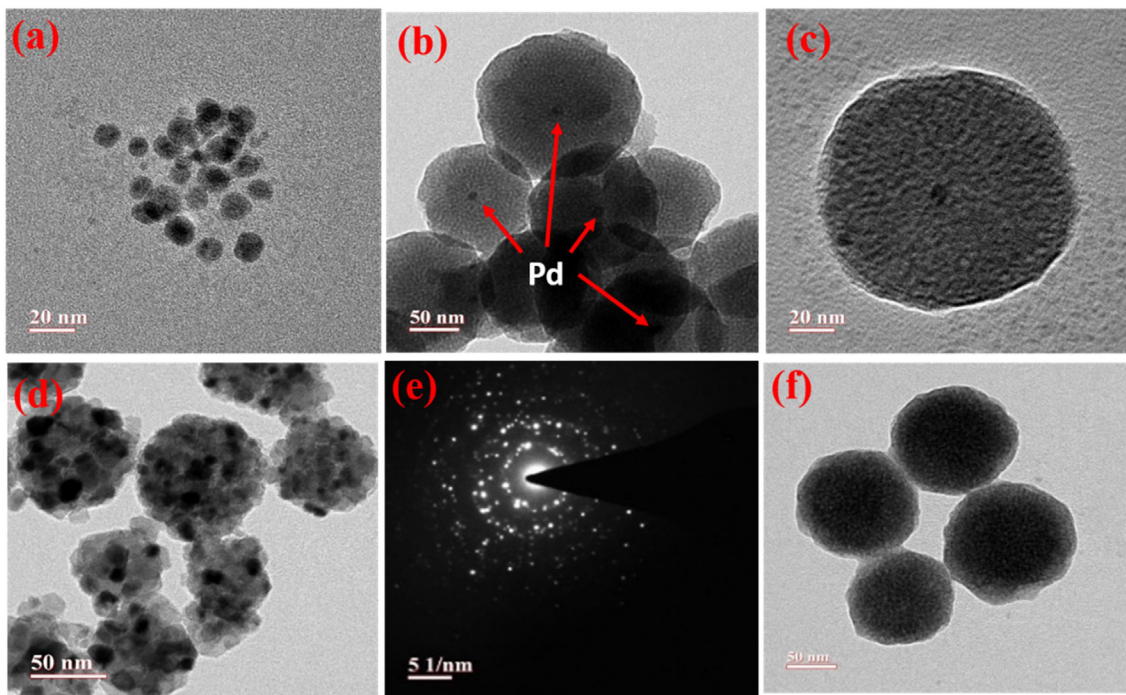


Fig.2. TEM images of (a) Pd NPs, Pd@ZnO CSNPs (b) before calcination, (c) enlarged single particle, (d) as-calcined at 500 °C (e) SAED pattern (f) ZnO NPs.

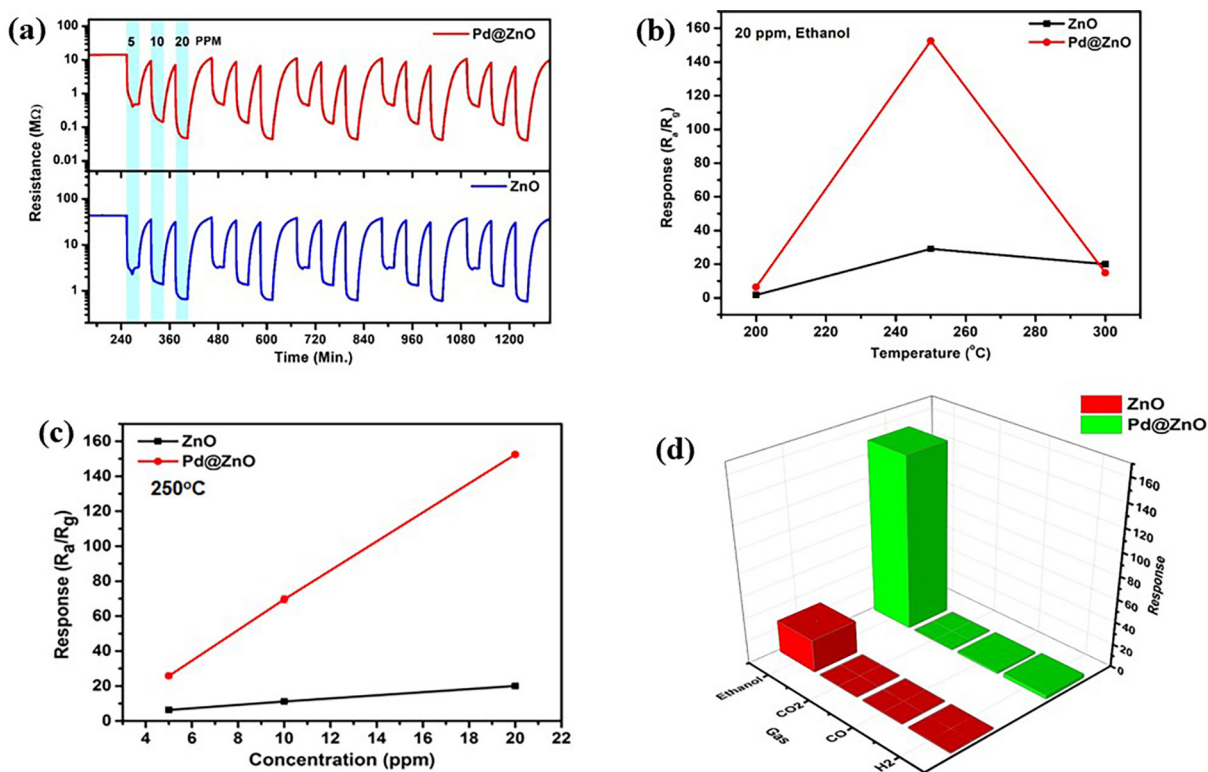


Fig. 3. Gas sensing results of ZnO NPs and Pd@ZnO CSNPs sensor (a) Sensor resistance behavior for ethanol (5, 10 and 20 ppm) at 250 °C and cycle was repeated 5 times (b) Temperature-dependent response towards 20 ppm ethanol (c) Response transient with varying ethanol concentration at 250 °C, and (d) response comparison tested to different gases at 250 °C.

for Pd@ZnO CSNPs in comparison to bare ZnO NPs toward ethanol vapors at 250 °C. This enhancement in the gas sensing performance is attributed to the electronic and chemical sensitization effects of Pd core NPs and their unique core@shell nanostructure. These

results suggest that Pd@ZnO CSNPs will be an ideal candidate for ethanol sensors having great potential in practical applications for real-time ethanol detection, such as fire detection or screening of drunken drivers.

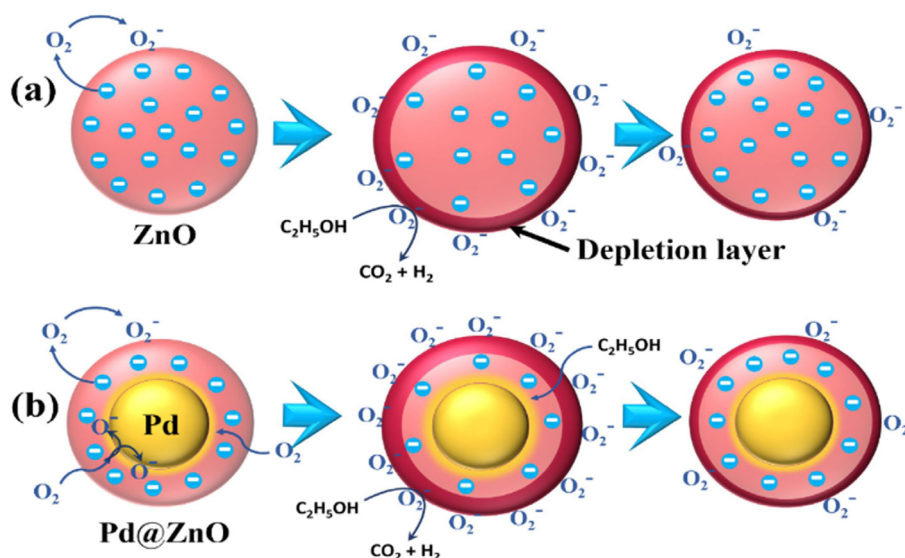


Fig. 4. The plausible gas sensing mechanism in the air and ethanol medium.

CRediT authorship contribution statement

Sonalika Agarwal: Conceptualization, Investigation, Visualization, Formal analysis, Writing - original draft. **Sanjay Kumar:** Formal analysis, Investigation, Writing - review & editing. **Eric Navarrete Gatell:** Investigation, Formal analysis, Writing - review & editing. **Manoj Kumar:** Validation, Writing - review & editing. **Eduard Llobet:** Resources, Writing - review & editing, Funding acquisition. **Kamlendra Awasthi:** Supervision, Project administration, Funding acquisition, Resources, Writing - review & editing.

Declaration of Competing Interest

The authors declare that they have no known competing financial interests or personal relationships that could have appeared to influence the work reported in this paper.

Acknowledgments

This work was supported by grant no. SR/WOS-A/PM-72/2016 and MRC, MNIT Jaipur. MICINN-FEDER and AGAUR funded part of this work via grants no. RTI2018-101580-and 2017SGR 418, respectively. E.N. gratefully acknowledges a doctoral fellowship from MINECO grant no. BES-2016-076582. E.L. is supported by the Catalan Institution for Research and Advanced Studies via the 2018 Edition of the ICREA Academia Award.

Appendix A. Supplementary data

Supplementary data to this article can be found online at <https://doi.org/10.1016/j.mblux.2021.100068>.

References

- [1] P. Cao, Z. Yang, S.T. Navale, S. Han, X. Liu, W. Liu, Y. Lu, F.J. Stadler, D. Zhu, *Sensors Actuators B Chem.* 298 (2019).
- [2] H. Zhang, J. Yi, *Mater. Lett.* 216 (2018) 196.
- [3] K.M. Tripathi, T.Y. Kim, D. Losic, T.T. Tung, *Carbon N. Y.* 110 (2016) 97.
- [4] Q. Li, D. Chen, J. Miao, S. Lin, Z. Yu, D. Cui, Z. Yang, X. Chen, *Sensors Actuators B Chem.* 326 (2021) 128952.
- [5] G. Ren, Z. Li, W. Yang, M. Faheem, J. Xing, X. Zou, Q. Pan, G. Zhu, Y. Du, *Sensors Actuators B Chem.* 284 (2019) 421.
- [6] X. Yang, H. Li, T. Li, Z. Li, W. Wu, C. Zhou, P. Sun, F. Liu, X. Yan, Y. Gao, X. Liang, G. Lu, *Sensors Actuators B Chem.* 282 (2019) 339.
- [7] S.K. Suar, S. Sinha, A. Mishra, S.K. Tripathy, *Handb. Res. Divers. Appl. Nanotechnol. Biomed. Chem. Eng.* 438 (2014).
- [8] S. Agarwal, L.K. Jangir, K.S. Rathore, M. Kumar, K. Awasthi, *Appl. Phys. A* 125 (2019) 553.
- [9] S.J. Park, G.S. Das, F. Schütt, R. Adelung, Y.K. Mishra, K.M. Tripathi, T.Y. Kim, *NPG Asia Mater.* 11 (2019).
- [10] L. Wang, Y. Kang, X. Liu, S. Zhang, W. Huang, S. Wang, *Sensors Actuators B Chem.* 162 (2012) 237.
- [11] Y. Zhao, S. Wang, W. Yuan, S. Fan, Z. Hua, Y. Wu, X. Tian, *Sensors Actuators B Chem.* 328 (2021).
- [12] T.T.D. Nguyen, H.N. Choi, M.J. Ahemad, D. Van Dao, I.H. Lee, Y.T. Yu, *J. Alloys Compd.* 820 (2020) 153133.
- [13] M. Yang, Y. Gong, G. Shen, Z. Wang, M. Liu, Q. Wang, *Mater. Lett.* 283 (2021) 128733.
- [14] R.J. Wu, D.J. Lin, M.R. Yu, M.H. Chen, H.F. Lai, *Sensors Actuators B Chem.* 178 (2013) 185.
- [15] Y.H. Zhang, X.L. Cai, L.Z. Song, F.Y. Feng, J.Y. Ding, F.L. Gong, *J. Phys. Chem. Solids* 124 (2019) 330.
- [16] S. Agarwal, P. Rai, E. Navarrete, E. Llobet, F. Güell, M. Kumar, K. Awasthi, *Sensors Actuators B Chem.* 292 (2019) 24.
- [17] S.M. Majhi, H.J. Lee, H.N. Choi, H.Y. Cho, J.S. Kim, C.R. Lee, Y.T. Yu, *CrystEngComm* 21 (2019) 5084.
- [18] X. San, D. Liu, G. Wang, Y. Shen, D. Meng, F. Meng, *Mater. Sci. Inc., Nanomater. Polym.* 4 (2019) 2694.
- [19] P. Rai, S.M. Majhi, Y.T. Yu, J.H. Lee, *RSC Adv.* 5 (2015) 76229.
- [20] M. Kaur, S. Kailasaganapathi, N. Ramgir, N. Datta, S. Kumar, A.K. Deb Nath, D.K. Aswal, S.K. Gupta, *Appl. Surf. Sci.* 394 (2017) 258.
- [21] H. Di Zhang, Y.Z. Long, Z.J. Li, B. Sun, *Vacuum* 101 (2014) 113.
- [22] X. Li, X. Zhou, H. Guo, C. Wang, J. Liu, P. Sun, F. Liu, G. Lu, *ACS Appl. Mater. Interfaces* 6 (2014) 18661.
- [23] P. Rai, J.W. Yoon, C.H. Kwak, J.H. Lee, *J. Mater. Chem. A* 4 (2015) 264.
- [24] T.T.D. Nguyen, D. Van Dao, I.H. Lee, Y.T. Yu, S.Y. Oh, *J. Alloys Compd.* 854 (2021) 157280.
- [25] L.-L. Xing, C.-H. Ma, Z.-H. Chen, Y.-J. Chen, X.-Y. Xue, *Nanotechnology* 22 (2011) 215501.